

# A Comparison of Error Estimators for Method of Moments

Charles Braddock  
 School of ECE  
 Georgia Institute of Technology  
 Atlanta, GA  
 cbraddock6@gatech.edu

Andrew Peterson  
 School of ECE  
 Georgia Institute of Technology  
 Atlanta, GA  
 afpeterson@gatech.edu

**Abstract**—Local error estimators are investigated for use with numerical solutions of the electric field integral equation. Three-dimensional test targets include a sphere, disk, NASA almond, and a Lockheed Martin Expedite aircraft model. Visual plots and correlation coefficients are used to assess the accuracy of the estimators. It is shown that the inexpensive discontinuity estimators are usually as accurate as the residual method.

**Keywords**—A posteriori error estimation, integral equations, method of moments, residuals.

## I. INTRODUCTION

The goal of a numerical approach is to be reliable and efficient [1]. To that aim, a posteriori error estimation has been used as a key method to assess the accuracy of computational solutions and to determine high error cells for  $h$ - and  $p$ -refinement [2]. For integral equations, the most widely used estimators are based on residual equations, which have a high computational cost. Error estimation schemes that take advantage of the discontinuity of the tangential current and charge density in the Rao-Wilton-Glisson (RWG) have been introduced that are as robust but much less computationally costly than a residual based error estimate [3], [4]. Strydom and Botha introduced charge and current recovery methods for the RWG that used smoothing procedures to determine more accurate solutions [5], [6]. In this work, modified versions of the discontinuity error estimators in [4], the recovery methods of [5] and [6], and a magnetic field tangential residual method are compared on PEC surfaces of a sphere, disk, almond, and Expedite model.

## II. ERROR ESTIMATOR EQUATIONS

### A. Tangential Current Discontinuity Estimator

The tangential current discontinuity error at the  $i^{\text{th}}$  cell is based on the average discontinuity of the surface current density at the midpoint of the three surrounding edges divided by two, normalized to twice the absolute value of the incident magnetic field:

$$LE_{J_{tan}}^i = \frac{\frac{1}{3} \sum_{m=1}^3 |\hat{t}_m \cdot (\vec{j}^i - \vec{j}^{n(i,m)})|}{2|\vec{H}^{inc}|} \frac{A_i}{A_{avg}}, \quad (1)$$

where  $\hat{t}_m$  is a unit vector tangential to the  $m^{\text{th}}$  edge of the  $i^{\text{th}}$  cell,

$n(i,m)$  is the adjacent cell that shares the  $m^{\text{th}}$  edge with the  $i^{\text{th}}$  cell,  $A_i$  is the area of the  $i^{\text{th}}$  cell, and  $A_{avg}$  is the average cell area of the mesh. The factor of one half in the numerator of (1) is motivated by the assumption that the true value of the tangential current is the average of the two calculated values. The normalization factor was chosen due to it being the theoretical maximum value of the current on a sphere. The maximum value of the discontinuities was not used so that large discontinuities from cells along edges do not overwhelm the calculations of other cells.

### B. Charge Discontinuity Error Estimator

The charge discontinuity error estimate at the  $i^{\text{th}}$  cell is of the form:

$$LE_{\rho}^i = \frac{\frac{1}{3} \sum_{m=1}^3 \frac{1}{2\epsilon} |\rho^i - \rho^{n(i,m)}|}{2|\vec{E}^{inc}|} \frac{A_i}{A_{avg}}, \quad (2)$$

where the same superscripts of  $i$  and  $n(i,m)$  are used as the tangential current discontinuity estimator. Each difference of the charge densities along an edge is divided by the epsilon of the surrounding space. The normalization constant, twice the absolute value of the incident electric field, is chosen because it is the theoretical maximum value of the charge density of a smooth sphere. The additional division by two comes from the same assumption as that in the tangential current discontinuity estimator.

### C. Current Weighted Charge Discontinuity Estimator

The current weighted charge discontinuity (CWCD) error estimator was introduced in [3] and uses the current density to modify the charge discontinuity estimator to obtain:

$$LE_{CWCD}^i = \frac{\frac{1}{3} \sum_{m=1}^3 \frac{1}{2} |k\eta(\vec{T}_m \cdot (\vec{j}^i + \vec{j}^{n(i,m)}))| + \frac{1}{2\epsilon} |\rho^i - \rho^{n(i,m)}|}{2|\vec{E}^{inc}|} \frac{A_i}{A_{avg}}. \quad (3)$$

The same superscripts of  $i$  and  $n(i,m)$  are used as the current discontinuity estimator.  $\vec{T}_m$  is the razor-blade test function across edge  $m$  from the  $i^{\text{th}}$  cell to the  $n(i,m)^{\text{th}}$  cell. The normalization constant of twice the magnitude of the incident electric field was chosen due to the common units being V/m.

This project was supported by Lockheed Martin Corp.

#### D. Magnetic Field Tangential Residual

The tangential H-field residual estimator is defined as:

$$LE_{HtanRes}^i = \frac{\sqrt{\sum_{m=1}^2 (\hat{t}_m \times (\bar{H}^{inc} + \bar{H}^s) - \bar{J}_s)_{cell i}^2}}{2|\bar{H}^{inc}|} * \frac{A_i}{A_{avg}}, \quad (4)$$

where  $\hat{t}_1$  and  $\hat{t}_2$  are orthogonal unit tangent vectors at the center of cell  $i$ , and the fields and current density are sampled at the center of cell  $i$ . The scattered field  $\bar{H}^s$  is computed from:

$$\bar{H}^s = \nabla \times \iint \bar{J}_s(u', v') G(u, v, u', v') du' dv', \quad (5)$$

which is imposed an infinitesimal distance outside the target surface. The estimator is limited to closed targets.

### III. TEST PROBLEMS

The error estimators in Section II and the recovery methods introduced in [5] and [6] where tested perfectly conducting targets including a sphere, a disk, a NASA almond, and an Expedite model (Fig. 1). The sources were uniform plane waves and the targets were modeled with triangular facets.

#### A. Sphere

The first test problem is a PEC sphere with radius  $\lambda$  with 648 fairly uniform and symmetric cells.

#### B. Disk

The disk is of approximate radius  $1.6\lambda$  with 516 cells. The incident plane wave is normally-incident to the disk plane.

#### C. NASA Almond

The NASA almond is of width  $2.5\lambda$  and length  $6\lambda$  with 640 cells. The incident plane waves used were horizontally (y) and vertically (z) polarized along the midline of the almond.

#### D. Expedite Model

The Expedite model, shown in Fig. 1, was provided by Lockheed Martin Corporation. It was of the length  $6\lambda$  and width  $5\lambda$  with 676 cells. The incident plane waves horizontally (y) and vertically (z) polarized.

### IV. RESULTS

For each test problem, visual models, global error estimates, scatter plots, and correlation coefficients as defined in [4] were generated. For the sphere and disk meshes, the results were compared to the true error values obtained from exact solutions. For the NASA Almond and Expedite meshes, the results were compared to the error values found by comparing to extrapolated values from much finer meshes. The local error is computed using:

$$LE_{ref}^i = \frac{\frac{1}{3} \sum_{m=1}^3 |\hat{n}_m (\bar{J}_{ref}^i - \bar{J}_{MoM}^i)|}{2|H_{inc}|} \frac{A_i}{A_{avg}}. \quad (6)$$

#### A. Global Error Estimate

The two-norm global error estimate was computed for each estimator. The two-norm global estimate was of the form:

$$GE_{2 Norm} = \sqrt{\frac{\sum A_n (LE_n \frac{A_{avg}}{A_n})^2}{\sum A_n}}, \quad (7)$$

where  $A_n$  is the area of the  $n^{th}$  cell and  $LE_n$  is the local error at the  $n^{th}$  cell.

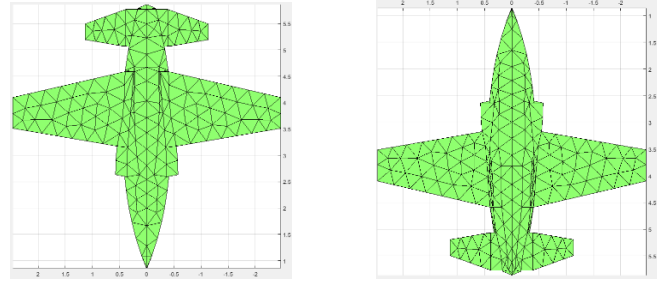


Fig. 1. 676 cell Expedite mesh viewed from the top and bottom of the mesh.

#### B. Correlation

The correlation coefficients between each estimator and the exact or reference error for each mesh are shown in Table I, following the definition in [7].

TABLE I. CORRELATION COEFFICIENTS

Geometry	Pol.	$J_t$	$\rho_e$	$CWCD$	$J_{rec}$	$\rho_{rec}$	Res $H_t$
Sphere	x	0.95	0.59	0.63	0.95	0.56	0.95
Disk	y	0.85	0.74	0.74	0.75	0.72	(NA)
Almond	y	0.85	0.88	0.89	0.84	0.87	0.87
Almond	z	0.29	0.26	0.33	0.16	0.24	0.30
Expedite	y	0.76	0.67	0.73	0.59	0.59	0.74
Expedite	z	0.47	0.43	0.49	0.44	0.39	0.75

#### C. Discussion

Based on the results shown above, it can be seen that for most cases the computationally cheaper discontinuity error estimation methods are just as accurate as the ‘‘industry standard’’ residual method.

### REFERENCES

- [1] A. F. Peterson, S. L. Ray, and R. Mittra, Computational Methods for Electromagnetics, New York, NY, USA: IEEE Press, 1998.
- [2] M. Ainsworth and J. T. Oden, A Posteriori Error Estimation in Finite Element Analysis, Hoboken, NJ, USA: Wiley, 2000.
- [3] J. Wang and J. P. Webb, ‘‘Hierarchical vector boundary elements and p-adaptation for 3-D electromagnetic scattering,’’ IEEE Trans. Antennas Propag., vol. 45, no. 12, pp. 1869-1879, Dec. 1997.
- [4] S. K. Kim and A. F. Peterson, ‘‘Evaluation of local error estimators for the RWG based EFIE,’’ IEEE Tans. Antennas Propagat., vol. 66, no. 2, pp. 819-826, Feb. 2018.
- [5] W. J. Strydom and M. M. Botha, ‘‘Charge recovery for the RWG-based method of moments,’’ IEEE Tans. Antennas Propagat. Letters, vol. 14, pp. 305-308, Oct. 2014.
- [6] W. J. Strydom and M. M. Botha, ‘‘Current recovery for the RWG-based method of moments,’’ IET Science, Measurement & Technology, vol. 10, no. 8, pp. 831-838, Nov. 2016.
- [7] S. K. Kim, ‘‘Error estimation and adaptive refinement technique in the method of moments,’’ Ph.D. dissertation, Dept. Elect. Comput. Eng., Georgia Inst. Technol., Atlanta, GA, USA, May 2017